RESEARCH PAPER

Acta Neurobiol Exp 2019, 79: 39–52
DOI: 10.21307/ane-2019-004

since 1928 ACTA NEUROBIOLOGIÆ EXPERIMENTALIS

The filled-space illusion induced by a single-dot distractor

Aleksandr Bulatov[1,2]*, Vilius Marma[1,2], Natalija Bulatova[2] and Lina Mickienė[2]

[1] *Laboratory of Visual Neurophysiology, Lithuanian University of Health Sciences, Kaunas, Lithuania,*
[2] *Institute of Biological Systems and Genetics Research, Lithuanian University of Health Sciences, Kaunas, Lithuania,*
* *Email: aleksandr.bulatov@lsmuni.lt*

In the present study, we tested the ability of our computational model of the filled-space illusion to account for data collected in experiments with stimuli comprising single-dot distractors. In three sets of experiments, we investigated this illusory effect as a function of distance between the distractor and lateral terminator of the reference spatial interval of the three-dot stimulus. We found that the model calculations properly predicted all of the observed changes in magnitude of the illusion for stimuli with a single distracting dot placed both within and outside the interval, as well as, for stimuli with two distractors arranged symmetrically relative to the lateral terminator. To additionally test the model, in a fourth set of experiments we performed psychophysical examination of the conventional Oppel-Kundt stimulus with a different number of equally spaced dots subdividing the filled part. Adequate correspondence between the computational and experimental data supports our assumptions concerning the origin of the filled-space illusion.

Key words: length misjudgment, filled-space illusion, Oppel-Kundt figure

INTRODUCTION

The filled-space illusion refers to perceptual overestimation of the length of a stimulus area filled with some contextual visual elements in comparison with an equivalent area that is empty. This visual phenomenon has been systematically studied for almost two centuries; however, at present there is no consensus about its origin. Although there are numerous modifications of the filled-space illusion, researchers have traditionally examined the metric distortions evoked by stimuli of the Oppel-Kundt type (Fig. 1D). In the Oppel-Kundt stimuli, there is a striking non-monotonic dependence of the effects of the illusion on the number of discrete filling elements. Previous studies (Obonai, 1933; Spiegel, 1937; Piaget and Osterrieth, 1953; Coren et al., 1976; Noguchi et al., 1990; Bulatov et al., 1997; Deregowski and McGeorge, 2006; Wackermann and Kastner, 2010; Giora and Gori, 2010; Mikellidou and Thompson, 2014) demonstrate that a stimulus with a certain number of evenly distributed identical fillers induces a considerably stronger illusion than stimuli with irregular fillers (Lewis, 1912; Noguchi, 2003) or continuous filling (Bailes, 1995; Bertulis and Bulatov, 2001). Interestingly, there is a substantial reduction in the Oppel-Kundt illusion in response to stimuli that are filled with elements that differ in shape or size (Obonai, 1954; Oyama, 1960; Wackermann and Kastner, 2009; Wackermann, 2012a), absolute luminance contrast (Bulatov and Bertulis, 2005), and color contrast under isoluminant conditions (Surkys, 2007). At the same time, the magnitude of the illusion has been shown to increase with figure/background luminance contrast (Long and Murtagh, 1984; Dworkin and Bross, 1998; Wackermann, 2012b). Many additional factors have been shown to affect the manifestation of the illusion. For instance, the magnitude of the illusion varies with the temporal duration of stimuli (Bailes, 1995; Dworkin and Bross, 1998), such that magnitude decreases with shorter stimulus presentations (Bertulis et al., 2014). The effects of the illusion

Received 14 May 2018, accepted 4 January 2019

exeley

are also considerably weaker in subjects who make voluntary saccadic eye movements during stimulus observations (Coren and Hoenig, 1972). Gaze fixation near the center of the filled portion of the stimulus leads to a significantly stronger illusion than when the gaze is directed towards the center of the empty spatial interval (Piaget and Bang, 1961).

Attempts to explain the filled-space illusion have resulted in various theories that are not as numerous as in the case of, for example, the Müller-Lyer illusion. These theories are primarily concerned with the effects caused by stimuli of the Oppel-Kundt type. According to the "psychophysical theory" proposed by Taylor (1962), the emergence of the filled-space illusion is associated with perceptual discriminability of the distance between different stimulus elements. In particular, if the stimulus elements are clearly discriminable then the apparent distances between them increase (thus, evoking the illusion). If the elements are not clearly discriminable, in contrast, then the distances may decrease. However, as noted by the author himself, this explanation requires additional assumptions that are not clearly defined, and include information from all available sources that an observer uses when making length judgments (Taylor, 1962). Another approach (Bertulis et al., 2014) suggests that the illusion may be related to perception of stimulus continuity. In particular, neural excitations individually evoked by fillers form a continuous path of activation (Smits et al., 1985; Beck et al., 1989; Field et al., 1993; Kojo et al., 1993; Hirsch et al., 1995), and the spatial extent of the activation determines the occurrence of the illusion. In contrast, the "contour density" hypothesis (Craven and Watt, 1989; Watt, 1990) considers the role of the number of zero-crossings (i.e., a measure of discontinuity) of the spatial profile of neural excitation in modulating the Oppel-Kundt illusion.

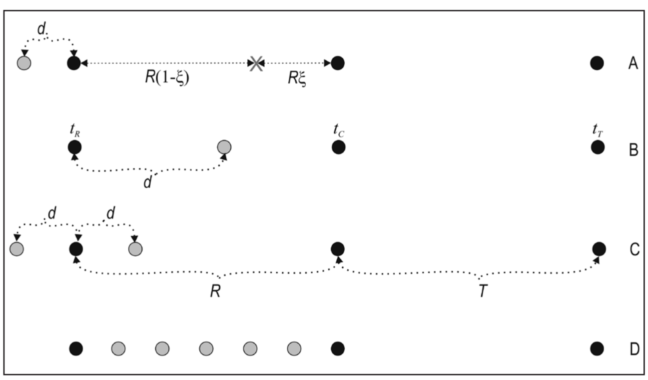

Fig. 1. Examples of stimuli used in the present study. The three-dot (t_R, t_C, and t_T) stimuli with a single distractor placed either outside (A) or inside (B) the reference interval. Two distracting dots (C) are presented symmetrically relative to the lateral stimulus terminator. *R* and *T*, the length of the reference and test interval, respectively; *d*, the distance between distractor and terminator; *ξ*, the coefficient determining the position of gaze fixation, *X*. (D) The conventional Oppel-Kundt stimulus with equally spaced distracting dots. For illustration purposes, the distractors are displayed in grey shading. However, in experiments, white stimuli (luminance of all the dots, 75 cd/m^2) were presented against a dark round-shaped background (5° in diameter and 0.4 cd/m^2 in luminance).

Together with qualitative explanations of the effects of the filled-space illusion (i.e., without at least minimal description of corresponding computational method), a number of quantitative theoretical approaches have been developed to account for the accumulated experimental data. Ganz (1966) suggested that lateral inhibition causes specific changes in the profiles of neural excitation, which may result in a perceptual repulsion of adjacent stimulus elements, thereby inducing the Oppel-Kundt illusion. Several investigators have applied the attraction/repulsion formalism of the electrical potential theory (Eriksson, 1970), or methods of "logarithmic information integration" (Erdfelder and Faul, 1994) into model calculations; others use functions that were composed to fit the experimental results (Wackermann and Kastner, 2010). As an example of another quantitative approach, a more physiologically plausible computational model of spatial-frequency filtering that involves properties of receptive fields of neurons in the primary visual cortex (Bulatov et al., 1997; Bulatov and Bertulis, 1999; 2005).

Recently, a preliminary quantitative model of the filled-space illusion was proposed (Bulatov et al., 2017) to determine whether perceptual positional biases induced by spatial pooling of context-evoked neural excitation are powerful enough to account for data obtained from experiments with stimuli comprising the continuous filling. The model calculations closely matched data collected using varied parameters of the horizontal three-dot stimulus (e.g., either length of a contextual line segment filling the reference interval, or the length of the reference interval while maintaining fixed length of the filling segment). In addition, the model was successfully applied to account for data acquired in experiments with conventional Oppel-Kundt figures. Although the proposed theoretical approach may be overly simplistic, the model provides a unified explanation for the experimental results accumulated for stimuli comprising both continuous and discrete filling elements, and thereby provides an interesting and potentially fruitful heuristic to guide further research. We assert that a more thorough exploration of illusion characteristics for a wider range of stimulus modifications can shed new light on issues concerning the features of the effect under study. More thorough study can also be helpful for developing a more comprehensive theoretical description of the illusion.

The aim of the present study was to further develop our model of the filled-space illusion. We examined whether model equations can be used to fit to experimental data obtained with the most elementary stimulus comprising single-dot distractors (Fig. 1). To this end, we performed three sets of psychophysical experiments to quantitatively determine the illusory effect as a function of distance between the distractor and lateral terminator of the reference spatial interval of the three-dot stimulus. In the first two sets of experiments, we used stimuli that comprised a single distracting dot placed either outside (Fig. 1A) or inside (Fig. 1B) of the reference interval. In the third set of experiments, a stimulus with two distractors arranged symmetrically relative to the lateral terminator (Fig. 1C) was used. To collect data on the conventional Oppel-Kundt stimulus (Fig. 1D), which consists of a varying number of equally spaced dots, a fourth set of experiments was performed with the same group of observers. The use of elementary stimuli made up of dots distributed along a single axis allowed us to reduce the number of unknown interfering factors and consider only the simplest one-dimensional effects of the filled-space illusion. This simplification facilitates the subsequent theoretical interpretation of the experimental results.

Description of the model

Despite the long history of investigations and large amount of accumulated experimental data, there is still insufficient evidence to identify the specific neuronal mechanisms responsible for the emergence of the filled-space illusion. In our previous study of stimuli with continuous filling (Bulatov et al., 2017), we proposed a simple computational model that represents hypothetical visual procedure of a weighted spatial pooling of neural excitations within limits of some attentional windows. According to the model, the process of length judgments is concerned with neural calculations based on information about visual coordinates of terminators of stimulus' spatial intervals (Bulatov et al., 2005). This information is subsequently encoded by the magnitude of integrated responses of relevant attentional windows, which are centered at the terminators. Assuming the same parameters for the circular Gaussian profiles of neural excitation and attentional window (which linearly increase in width with retinal eccentricity), the magnitude (S) of the response evoked by a single dot presented at eccentricity (ρ) can be evaluated as follows:

$$S(\rho,k,s)=\iint_{\infty} e^{-\frac{x^2+y^2}{(k\rho+s)^2}}dxdy=\pi\left(k\rho+s\right)^2=\pi\sigma\left(\rho,k,s\right)^2, \tag{1}$$

where k represents the slope and s represents the intercept of the linear regression of the standard deviation, $\sigma(\rho,k,s)$ of the Gaussian function of attentional window. To provide initial amplitude-independent conditions, this model assumes the procedure of the normalization (in our case, simple scaling the input excitation amplitude to the range 0-to-1) of neural activity that is known to play an important role in information processing at different levels of the nervous system (Reynolds and Heeger, 2009; Olsen et al., 2010, Carandini and Heeger, 2012; Vokoun et al., 2014).

In addition, the presence of a contextual distractor in the vicinity of the stimulus terminator can be considered to be a source of an additional distorting signal (S_{add}). Due to increased cumulative response of relevant attentional windows, S_{add} adds perceptual bias in the assessment of the coordinates of this terminator and thus causes misjudgments in a length-matching task. Assuming that increased signaling is interpreted by the visual system as a shift in perceived localization (i.e., $S(\rho+\delta,k,s)=S(\rho,k,s)+S_{add}$), the bias ($\delta$) evoked by the distractor can be easily derived from formula 1 and assessed as follows:

$$\delta=\frac{\sqrt{S(\rho,k,s)+S_{add}}-\sqrt{S(\rho,k,s)}}{k\sqrt{\pi}}\text{, and, for } S_{add} \ll S(\rho,k,s),\ \delta\approx\frac{S_{add}}{2k\sqrt{\pi S(\rho,k,s)}}=\frac{S_{add}}{2k\pi\sigma(\rho,k,s)}. \tag{2}$$

An interesting consequence of this assumption is that the illusion should manifest for stimuli wherein the distracting dot is placed both outside (Fig. 1A) and inside (Fig. 1B) of the reference interval. The illusion should be approximately twice as large in the case of two distractors (Fig. 1C) arranged symmetrically with respect to the lateral terminator. This is due to the roughly symmetrical spatial pooling of neural excitation within the terminator-related attentional window.

Accounting for the effects of varying gaze direction, the two-dimensional spatial profile of additional excitation evoked by distracting dots can be described by the positive part of the function:

$$F(x,y,d,k,s,\xi) = I_{out} e^{-\frac{(x+d)^2+y^2}{2\sigma(R(1-\xi)+d,k,s)^2}} + I_{in} e^{-\frac{(x-d)^2+y^2}{2\sigma(R(1-\xi)-d,k,s)^2}} - (I_{out}+I_{in}) e^{-\frac{x^2+y^2}{2\sigma(R(1-\xi),k,s)^2}} - I_{in} e^{-\frac{(x-R)^2+y^2}{2\sigma(R\xi,k,s)^2}}, \quad (3)$$

where ξ is the coefficient determining the position of gaze fixation (Fig. 1); R and d represent the length of the reference interval and the distance between the lateral terminator and distractor (i.e., distractor shift), respectively; I_{out} and I_{in} are the binary coefficients defining the presence (I=1) or absence (I=0) of corresponding distractor. In turn, the positive part of function 3 can be obtained using the following formula:

$$P(x,y,d,k,s,\xi) = F(x,y,d,k,s,\xi)H(F(x,y,d,k,s,\xi)), \quad (4)$$

where H(.) represents the Heaviside step function.

Adhering to the assumption regarding the same parameters for Gaussian functions of relevant attentional windows and excitation profiles, the magnitude of the cumulative response from the window (A_R) centered at the lateral terminator (t_R) of the reference interval can be therefore evaluated (Fig. 2A) as follows:

$$Z_R(d,k,s,\xi) = S(R(1-\xi),k,s) + \iint_\infty A_R P(x,y,d,k,s,\xi)dxdy = S(R(1-\xi),k,s) + \iint_\infty e^{-\frac{x^2+y^2}{2\sigma(R(1-\xi),k,s)^2}} P(x,y,d,k,s,\xi)dxdy \cdot \quad (5)$$

Similarly, the cumulative response from the attentional window (A_C) centered at the terminator (t_C), can be evaluated as follows:

$$Z_C(d,k,s,\xi) = S(R\xi,k,s) + \iint_\infty A_C P(x,y,d,k,s,\xi)dxdy = S(R\xi,k,s) + \iint_\infty e^{-\frac{(x-R)^2+y^2}{2\sigma(R\xi,k,s)^2}} P(x,y,d,k,s,\xi)dxdy. \quad (6)$$

Of note, by determining the location of the zero-crossings of function 3, the integration procedure can be easily performed analytically. However, the resulting expressions are too long and do not provide any additional information that warrant presentation in this manuscript.

Next, according to formula 2, the magnitude of the illusion (i.e., overestimation of the length of the filled reference stimulus interval in comparison with that of the empty test one) as a function of the distance (d) between the lateral terminator and distracting dot can be described using the following formula:

$$\Delta(d,k,s,\beta,\xi) = \delta_R + \beta\, sign(\xi)\,\delta_C = \frac{\sqrt{Z_R(d,k,s,\xi)} - \sqrt{S(R(1-\xi),k,s)}}{k\sqrt{\pi}} + \beta\, sign(\xi) \frac{\sqrt{Z_C(d,k,s,\xi)} - \sqrt{S(R\xi,k,s)}}{k\sqrt{\pi}}, \quad (7)$$

where *sign* (ξ) represents the sign function for the coefficient ξ. Of note, coefficient ξ is positive in the case of the gaze fixated within the reference interval, and negative for instances in which the fixation is within the test interval. The value of the coefficient (β) depends on the pattern of involuntary eye movements and gaze fixation during perceptual judgment and decision-making (Krauzlis et al., 2017), and reportedly falls between the values of 0 and 2. The presence of a distractor within the reference interval causes bias (δ_C) in the central terminator that changes the perceived length of both the reference and test intervals of the stimulus. In cases wherein the subjects hold their gaze fixed within one of the intervals (either reference or test), the observed bias is the sum of two contributions (each with the same sign) that influence the magnitude of the illusion. In those cases, the value of the coefficient β can reach 2. In contrast, if the subjects' gaze is approximately equally allocated to each of the intervals, then the contributions of the central terminator bias largely compensate each other. Equal gaze allocation should therefore result in a coefficient β that is around zero.

The proposed principle of model calculations can be extended to some other patterns with different spatial structures. For instance, in the case of the stimulus with equally spaced dots in the reference interval (i.e., the conventional Oppel-Kundt figure, Fig. 1D) the corresponding two-dimensional profile of neural excitation can be described as follows (Bulatov et al., 2017):

$$\Omega(x, y, n, k, s, \xi) = \sum_{i=0}^{i=n+1} e^{-\frac{\left(x-\frac{iR}{n+1}\right)^2+y^2}{2\sigma\left(R(1-\xi)-\frac{iR}{n+1},k,s\right)^2}}, \qquad (8)$$

where n represents the number of filling dots; and R is the length of the interval. Next, the spatial profile of additional signaling can be evaluated using the positive part of the following function:

$$F_{\Omega}(x, y, n, k, s, \xi) = \frac{\Omega(x, y, n, k, s, \xi)}{M(n, k, s, \xi)} - e^{-\frac{x^2+y^2}{2\sigma(R(1-\xi),k,s)^2}} - e^{-\frac{(x-R)^2+y^2}{2\sigma(R\xi,k,s)^2}}, \qquad (9)$$

where $M(n,k,s,\xi)$ is used to normalize neural excitation and represents peak values for function 8; unfortunately, an assessment of these peak values can be performed only numerically. The following steps in calculations are identical to those given in formulas (4) – (7).

Fig. 2 shows the calculated alterations of the illusion magnitude as a function of the distractor shift. The model calculations predict a relatively simple shape of curves with a single maximum (Fig. 2B) for stimulus that comprises a single distracting dot positioned outside the reference interval. As can be seen from the graphs, the magnitude of the maximum and its location depend considerably on the gaze direction (the value of coefficient, ξ). This dependence is also true for stimuli both with a single distractor placed within the reference interval (see Fig. 2C) and two dots located symmetrically with respect to the lateral terminator (Fig. 2D). However, the shape of the calculated curves becomes more complex due to the appearance of addi-

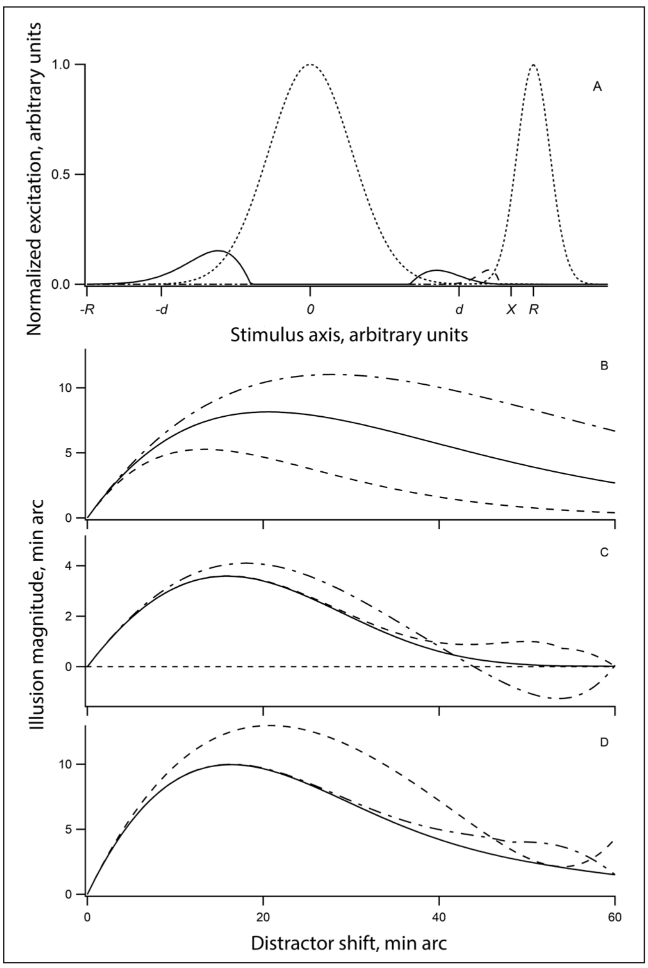

Fig. 2. Diagrams illustrating the model calculations. (A) The dotted curve represents the normalized profile of excitation caused by the lateral (located at 0) and central (located at R) stimulus terminators. Solid and dashed curves represent the profiles of additional excitation, caused by two symmetrically arranged distractors located at –d and d. This excitation is related to attentional windows centered at the lateral and central terminators, respectively; X, represents the position of gaze fixation. The model predictions, provided in formula 7, define the magnitude of the illusion as a function of the shift of distractors placed outside (B, gaze fixation parameters: ξ=0, solid; ξ=0.5, dashed; ξ=-0.5, dash-dot; β=0), or inside the interval (C, gaze fixation parameters: ξ=0, solid; ξ=0.1, dashed; ξ=-0.1, dash-dot; β=0.5), or arranged symmetrically (D, gaze fixation parameters: ξ=0, solid; ξ=0.2, dashed; ξ=-0.2, dash-dot; β=1). Calculations used the slope (k=0.2) and intercept (s=5 arcmin), which specify the linear dependence on eccentricity for the standard deviation of the Gaussian profile of attentional windows. Length of the reference interval (R) was equal to 60 arcmin.

tional extremum points or plateau when the distractor approaches the central terminator, given that the illusion magnitude also depends on perceptual biases of the central terminator.

For the sake of simplicity, our model considered only the simplest ways of viewing the stimuli. This is in contrast to real experimental conditions, wherein the observations occur without any strict limitations regarding the direction of gaze fixation, saccades, attentional shifts, etc. Since the values of the perceptual biases caused by contextual distractors strongly depend on retinal eccentricity of stimulus elements, the illusion magnitude may vary with shifts in the direction of the observer's gaze. Nonetheless, we expected that model calculations and measured values of the illusion magnitude would be correlated, on average.

METHODS

Apparatus

The experiments were carried out in a dark room (surrounding illumination <0.2 cd/m^2). A Sony SDM-HS95P 19-inch LCD monitor (spatial resolution 1280×1024 pixels, frame refresh rate 60 Hz) was used for stimulus presentation. A Cambridge Research Systems OptiCAL photometer was applied to the monitor luminance range calibration and gamma correction. A chin and forehead rest was used to maintain a constant viewing distance of 330 cm (at this distance each pixel subtended about 0.3 arcmin). An artificial pupil, which is an aperture with a 3 mm diameter of a diaphragm placed in front of the eye, was applied to reduce optical aberrations.

Stimuli were presented in the center of a round-shaped background of 5º in diameter and 0.4 cd/m^2 in luminance. Of note, the monitor screen was covered with a black mask with a circular aperture to prevent observers from being able to use the edges of the monitor as a vertical/horizontal reference. For all stimuli drawings, the Microsoft GDI+ antialiasing technique was applied to avoid jagged-edge effect.

Stimuli

The stimuli used in the experiments consisted of three horizontally arranged dots (diameter, 1 arcmin; luminance, 75 cd/m^2), which were considered to be terminators (t_R, t_C, and t_T; see Fig. 1) that specified the ends of the reference and test stimulus intervals. The length of the reference interval (R) was fixed at 60 arcmin.

In the first three set of experiments, the distance, (d, the independent variable) between the distracting dot (diameter, 1 arcmin; luminance, 75 cd/m^2) and the lateral terminator (t_R) was varied randomly from 0 to 60 arcmin. In the first and the second set of experiments, a single distractor was placed outside (Fig. 1A) and within (Fig. 1B) the reference interval, respectively. In the third set of experiments, two distracting dots were presented symmetrically with respect to the lateral stimulus terminator (Fig. 1C).

In the fourth set of experiments, the reference interval (length, 60 arcmin) was filled with a set of equally spaced dots (diameter, 1 arcmin; luminance, 75 cd/m^2) according to the conventional Oppel-Kundt pattern (Fig. 1D). The number of filling dots varied randomly from 0 to 30.

Procedure

To establish the functional dependences of the illusion magnitude on different spatial parameters of the stimulus, we used an adjustment method. During the experimental run, subjects were asked to manipulate the keyboard buttons "←"and "→" to move the lateral terminator (t_T) of the test interval to a position that makes both stimulus parts perceptually equal in length (see Fig. 1). The physical difference between the lengths of the test and reference intervals ($T-R$) was considered as the value of the illusion magnitude. A single button push varied the position of the terminator by one pixel, corresponding to approximately 0.3 arcmin. The initial length differences between the stimulus intervals were randomized and distributed evenly within a range of ±10 arcmin.

Subjects were encouraged to maintain their gaze on the central stimulus terminator; however, observation time was not limited and eye movements were not recorded. Each experimental run consisted of two types of stimulus presentation condition. In the first condition, the reference (i.e., filled) interval was presented on the left side of the stimulus. In the second condition, the reference was on the right side of the stimulus. Trials from different conditions were randomly interleaved to minimize effects of the left/right visual field anisotropy, and to reduce stimulus persistence. An experimental run consisted of 124 stimulus presentations. During each run, 31 different values of the independent variable for each stimulus condition were presented twice each, in a pseudo-random order. Each observer carried out at least five experimental runs on different days. The method of least squares was used to fit the experimental data (*genfit* function, Matlab MathWorks).

Subjects

Data were collected from four experienced human observers (UL, AK, LE, and RV) who previously took part in similar psychophysical studies. The subjects (with the exception one of the authors, UL) were naïve with respect to the purpose of the study, and all had normal or corrected-to-normal vision. To provide more standardized viewing conditions (for example, eliminating potential effects related to binocularity), the right eye was always tested irrespective of whether it was the leading eye or not. All subjects provided their informed consent before taking part in the experiments performed, in accordance with the ethical standards of the Declaration of Helsinki.

In addition, stimuli from the first three sets of experiments were tested with a group of inexperienced observers; in particular, University students (19–21 years of age, five females) during their elective course of cognitive psychology. However, the experimental conditions for these subjects were significantly less strict. In particular, we used: free binocular viewing under standard classroom illumination; no fixation of head position; and an average eyes-to-monitor distance of about 70 cm, resulting in an angular length of the reference stimulus interval of approximately 280 arcmin. Therefore, the data collected in inexperienced observers are mostly illustrative.

RESULTS

Experimental data

The aim of the first set of experiments was to determine quantitatively the magnitude of the filled-space illusion as a function of distance between the lateral terminator and a single distractor placed outside the reference spatial interval. As can be seen from the graphs shown in Fig.3, experimental results from all subjects yielded curves of similar shape. The illusion magnitude rapidly increased to its maximum value (5-8 arcmin), with increasing the distance between the terminator and distractor up to about 12-16 arcmin. Afterwards, the magnitude decreases gradually to about 0-2 arcmin for contextual distractors positioned at the distance of 60 arcmin from the lateral terminator.

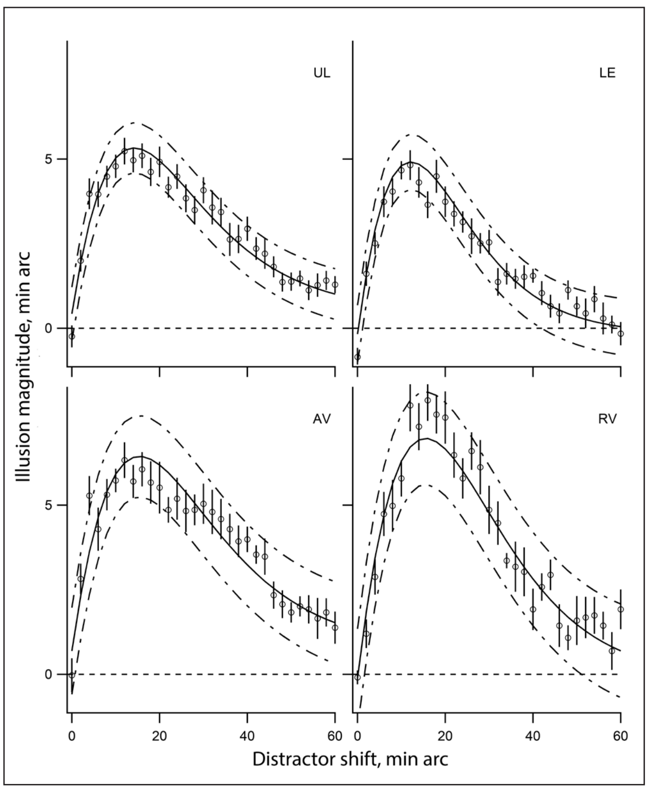

Fig. 3. The illusion magnitude as a function of shift of a distractor placed outside the reference interval. Solid curves represent the least squares fittings of function 10 to the experimental data (circles); dash-dot curves depict confidence intervals of the fitting; error bars represent ± one standard error of the mean (SEM). Subjects: UL, LE, AV, and RV.

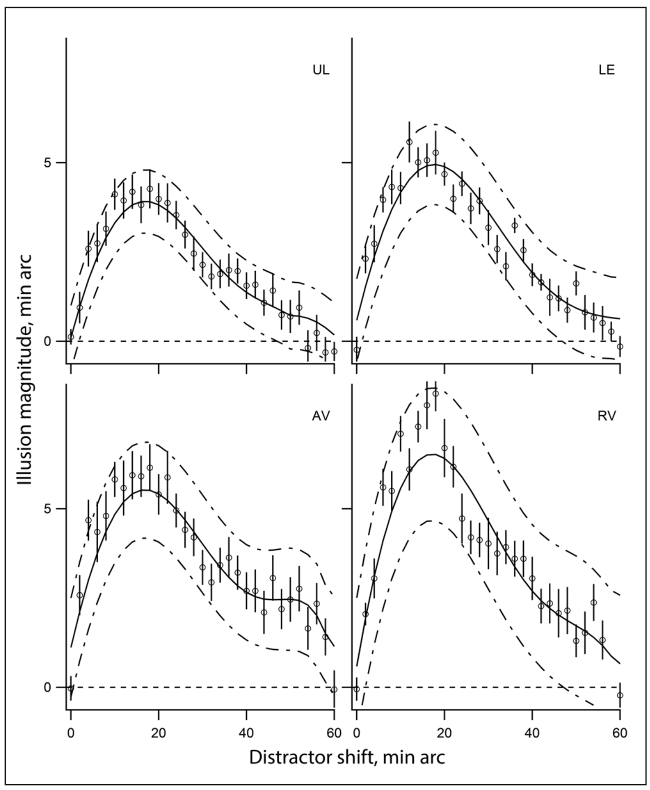

Fig. 4. The illusion magnitude as a function of shift of a distractor placed inside the reference interval. Solid curves represent the least squares fittings of function 10 to the experimental data (circles); dash-dot curves depict confidence intervals of the fitting; error bars represent ± one standard error of the mean (SEM). Subjects: UL, LE, AV, and RV.

In the second set of experiments, a single distracting dot was placed within the reference interval, and its position relative to the lateral terminator randomly varied from 0 to 60 arcmin. According to model predictions, we expected functional dependence, with parameters similar to those obtained in the first set of experiments. We expected the only difference from the first set of experiments to be that the curves may become more complex due to the appearance of additional extremum points or plateau (due to putative perceptual biases of the central stimulus terminator). As shown in Fig. 4, across all subjects, the illusion magnitude quickly increased and reached a maximum (4-8 arcmin) at the distance between distractor and terminator of about 15-18 arcmin. Thereafter, the illusion gradually weakened and its magnitude approached zero when the distracting dot coincided with the central terminator of the stimulus. In some cases (e.g., subject AV), the slope of the experimental curve clearly decreased and remains close to zero for distractor positions ranging from 40-55 arcmin (i.e., when approaching the central stimulus terminator).

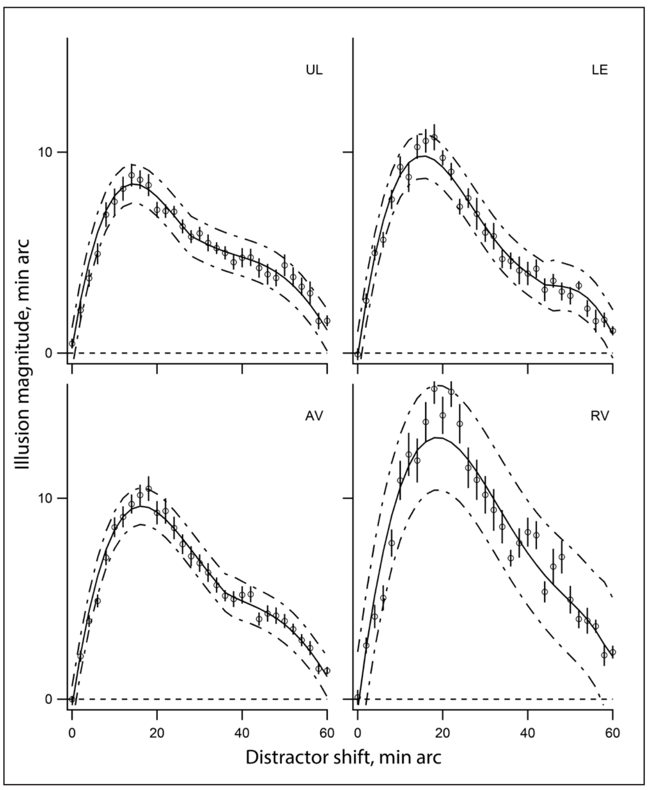

Fig. 5. The illusion magnitude as a function of shift of distractors that are arranged symmetrically relative to the lateral terminator. Solid curves represent the least squares fittings of function 10 to the experimental data (circles); dash-dot curves depict confidence intervals of the fitting; error bars represent ± one standard error of the mean (SEM). Subjects: UL, LE, AV, and RV.

In the third set of experiments, two distracting dots arranged symmetrically with respect to the lateral stimulus terminator were used (Fig. 1C). Of note, the distance between the distractors and the terminator randomly varied from 0 to 60 arcmin. As expected via model predictions, for all the subjects, the experimental curves (Fig. 5) showed that the magnitude of the illusion was almost two times larger than what was observed in the first two sets of experiments. In addition, for three subjects (UL, LE, and AV), we observed a tendency for some plateaus to emerge on the experimental curves; a plateau is evident when the distractor, placed

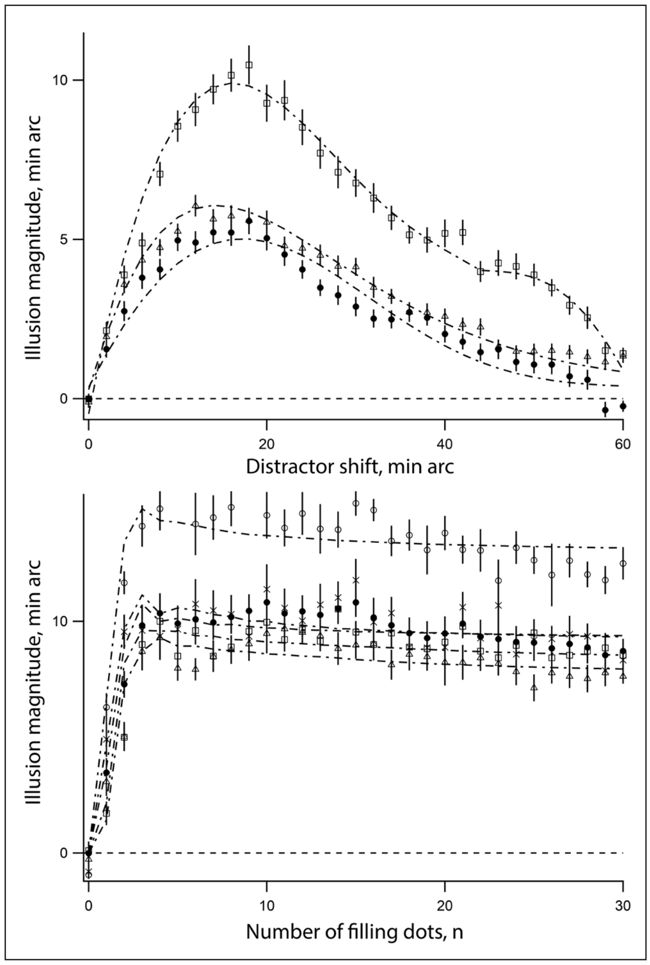

Fig. 6. The results of the fittings of the model function to the experimental data. In the upper graphs, the symbols represent grand means of the individual subject data, pooled across all four subjects. Grand mean data are shown as a function of shift of the distractors placed outside (triangles) or inside (closed circles) the reference interval, or arranged symmetrically relative to the lateral terminator (squares). In the lower graphs, the symbols represent the magnitude of illusion as a function of number of filling dots in the reference part of the Oppel-Kundt figure. Subjects: UL (squares), LE (triangles), AV (crosses), and RV (circles); grand means of the individual data for all four subjects (closed circles). Dash-dot curves represent the fittings of function 10 to the experimental data; error bars depict ± one standard error of the mean (SEM).

within the reference interval, approaches the central stimulus terminator.

To assess general trends of the results for the entire group of the observers, we calculated overall (i.e., grand) mean curves (Fig. 6, upper) from the individual experimental data. Relatively small SEM grand means values (e.g., not exceeding 0.37, 0.42, and 0.64 arcmin for data collected in the first, second, and third set of experiments, respectively) suggests similarity across individual experimental data sets.

The fourth set of experiments was conducted with the same group of observers to establish the dependence of the filled-space illusion magnitude on the number of filling dots (i.e., conventional Oppel-Kundt illusion), and additionally evaluate the applicability of our model. The experimental data curves are shown in the lower portion of Fig. 6. These curves are similar to those observed in previous studies of the Oppel-Kundt illusion (Coren et al., 1976; Bulatov et al., 1997; Deregowski and McGeorge, 2006; Wackermann and Kastner, 2010; Wackermann 2012a; 2012b). When the number of dots increased up to about 4-6, the magnitude of the illusion quickly reached a weakly expressed region of the maximum, and then slightly decreased to a relatively constant value (8-12 arcmin), with further increasing of subdivision density. Similar to data collected in the prior set of experiments, a grand mean curve was calculated from individual experimental results (see Fig. 6, lower, closed circles). The SEM grand mean curve values did not exceed 0.88 arcmin.

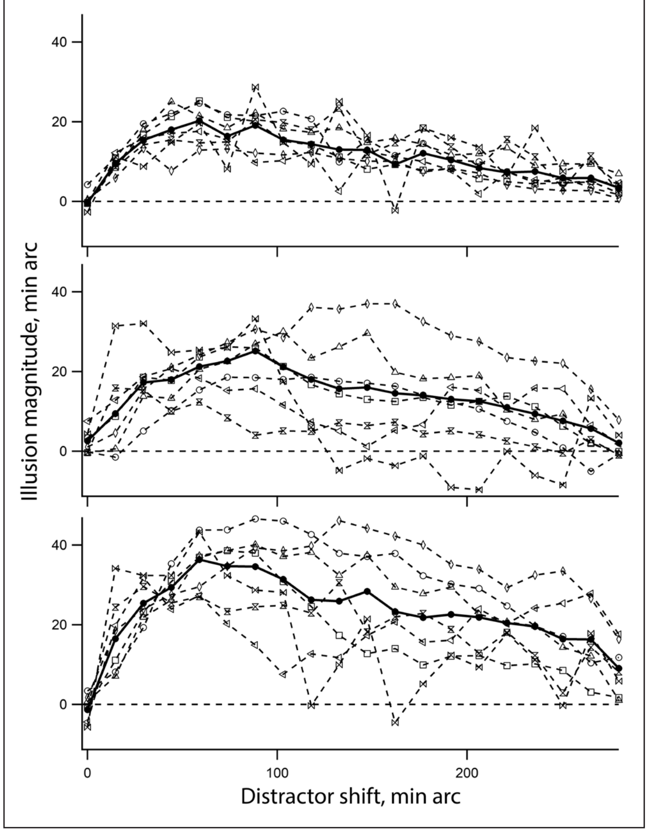

Fig. 7. Dependency of the illusion magnitude on the shift of distractors. In the graphs, dashed curves with different symbols represent the individual effects for seven subjects as a function of the shift of distractors placed outside (upper), or inside the reference interval (middle), or arranged symmetrically relative to the lateral terminator (lower). Thick solid curves represent grand means of the individual subject data. The length of the reference stimulus interval equal to 280 arcmin.

As noted in the Methods section, stimuli from the first three set of experiments were additionally tested with a group of inexperienced observers (University students). As can be seen from Fig. 7, there are relatively large inter-individual differences in the grand mean curves. Despite this large variation, the experimental data are similar to those shown in the upper graphs of Fig. 6, obtained in experienced observers. Although only qualitative, the similarity in curves obtained between inexperienced and experienced observers is further confirmation of our model.

Data fitting

The model calculations of the illusion magnitude are associated with use of a considerable number of free parameters (i.e., k, s, ξ, and β in formula 7) that relate to gaze fixation and the size of relevant attentional windows. Unfortunately, free parameters can significantly affect the reliability of theoretical predictions. Therefore, to examine performance of our model when the number of free parameters is reduced, we used several sequential steps to fit the data from different sets of experiments. Given that the highest number of influencing factors corresponds to the data obtained in the third set of experiments (with two distracting dots presented simultaneously), we fit those data (shown in Fig. 5) with the following function:

$$I(d) = C + \Delta(d, k, s, \xi, \beta)\,. \qquad (10)$$

Of note, the function has five free parameters, wherein C refers to a constant shift along the ordinate axis, and $\Delta(d,k,s,\xi,\beta)$ represents function 7. The values obtained for each subject for k and s were used in model fittings for the data collected in the second set of experiments (Fig. 4). Of note, there were three free parameters in function 10: C, ξ, and β. Thereafter, only two free parameters (C and ξ) were used in fittings of

 Acta Neurobiol Exp 2019, 79: 39–52

the data (Fig. 3) collected in the first set of experiments (Fig. 3), given that we did not need to take into account effects associated with the central attentional window (i.e., β=0). These processes were repeated on the grand mean data (Fig. 6, upper).

There was good correspondence in results of computational and experimental analyses (see Fig. 3-5, solid curves). Indeed, the coefficient of determination (R^2) in all cases was higher than 0.86 (Table I).

To more thoroughly examine goodness-of-fit, we applied the Shapiro-Wilk test, which test the normality of residuals (Table I). For each calculated curve, a matrix of partial derivatives of the model's function was multiplied by the residual mean square. These data allowed for an additional evaluation of the goodness-of-fit by calculating confidence intervals for predicted values at each point along the range of the independent variable (see Fig. 3-5, dash-dot curves).

As noted in the model description section, an assessment of peak values for function 8 can be performed only numerically; therefore, we used a manual fitting procedure on the data collected with the Oppel-Kundt stimulus. We used data collected in the third series of experiments to set the values for k and s of function 10. The free parameters in this function (C, ξ, and β) were manually adjusted within physiologically reasonable ranges to obtain the highest coefficient of determination (R^2; Fig. 6B, lower, dash-dot curves; Table I).

DISCUSSION

The proposed relatively simple theoretical approach does not claim to be a comprehensive explanation for the mechanisms underlying the emergence of the filled-space illusion. However, the model calculations

Table I. The resulting parameters of fitting Eqn. 10 to experimental data.[1]

Stimulus type	Parameters	Subjects				
		UL	LE	AV	RV	Grand mean
Symmetrical distractors	C	0.25±0.46	-0.14±0.58	-0.33±0.44	-0.5±1.4	-0.47±0.52
	k	0.22±0.02	0.19±0.02	0.2±0.01	0.17±0.03	0.19±0.01
	s	6.69±0.67	5.33±1.73	7.07±1.02	6.74±2.25	5.96±1.08
	ξ	0.54±0.07	0.27±0.17	0.4±0.09	0.03±0.26	0.27±0.11
	β	0.73±0.22	0.69±0.5	0.6±0.3	0.28±0.57	0.86±0.39
	R^2	0.97	0.98	0.98	0.93	0.98
	W, P_w	0.97, 0.58	0.99, 0.96	0.95, 0.19	0.98, 0.86	0.94, 0.11
Distractor inside	C	0.1±0.27	0.59±0.39	1.12±0.45	0.59±0.65	0.36±0.35
	ξ	0.17±0.08	-0.08±0.11	0.03±0.13	0.03±0.19	-0.13±0.09
	β	0.23±0.2	0±0.18	0.39±0.24	0.15±0.21	0±0.16
	R^2	0.92	0.91	0.87	0.88	0.93
	W, P_w	0.97, 0.61	0.96, 0.34	0.96, 0.35	0.97, 0.59	0.94, 0.07
Distractor outside	C	0.43±0.3	-0.17±0.29	0.69±0.49	-0.11±0.55	0.29±0.23
	ξ	0.65±0.05	0.58±0.05	0.56±0.08	0.39±0.09	0.5±0.04
	R^2	0.95	0.94	0.89	0.93	0.98
	W, P_w	0.99, 0.97	0.98, 0.91	0.96, 0.34	0.95, 0.13	0.98, 0.44
Oppel-Kundt	C	0	-0.17	-0.78	-0.25	-0.53
	ξ	0.54	0.49	0.4	0.8	0.62
	β	1.34	1.2	1.8	1.9	1.7
	R^2	0.87	0.86	0.85	0.91	0.92
	W, P_w	0.98, 0.79	0.95, 0.2	0.97, 0.57	0.99, 0.95	0.98, 0.91

[1] C (min of arc), a constant component; k and s (min of arc), the slope and intercept specifying eccentricity scaling for the standard deviation of the Gaussian profile of attentional windows; ξ and β, coefficients determining the gaze fixation parameters; R^2, coefficient of determination; W and P_w, the Shapiro-Wilk test statistic and p-value, respectively.

offer reasonable values of the illusion magnitude and also follow closely reported changes in the illusion induced by changing stimulus parameters. The data collected from the entire observer group demonstrate that the theoretical predictions fit all variations of the illusion magnitude as a function of distance between the lateral terminator and distracting dots placed outside/inside the reference spatial interval (Figs 3-5; Table I). Our results also confirmed the applicability of our model to data collected in experiments with conventional Oppel-Kundt figures that consist of a varying number of filling dots (Fig. 6, lower; Table I). Thus, our data are consistent with the idea that the context-evoked increase in neural excitation induces biases in perceptual localization of stimulus terminators, and these apparent displacements may be one of the main causes of the filled-space illusion (Bulatov et al., 2017).

According to our model, the magnitude of the illusion depends strongly on the size of terminator-related attentional windows and relevant profiles of neural excitation. These parameters are directly associated, in turn, with the gaze-fixation pattern during stimulus observation. This feature makes our approach in line with the following statement by Robinson (1998, p. 168) in his comprehensive review of visual illusions: “to be successful, a theory must deal with eye movements and fixation and must either show what contribution they make or demonstrate that they are irrelevant”. On the other hand, our model considered only the simplest forms of stimulus observations with single fixations. Nonetheless, even for simple forms, accounting for observed effects significantly complicates the calculations and requires a considerable number of free parameters to fit the experimental data.

We acknowledge that the proposed theoretical approach is simple, and represents only an initial step towards a more elaborate quantitative description of the phenomenon under study. For instance, one of the most important assumptions used in the calculations is related to the procedure of normalizing neural activity. In the model, we implemented an extremely straightforward method of signal scaling between 0 and 1. Most of the literature, in contrast, uses a more complicated procedure of a “divisive normalization” (Reynolds and Heeger, 2009; Olsen et al., 2010; Carandini and Heeger, 2012; Vokoun et al., 2014). At the same time, the proposed simple method of normalization can be justified, in part, by experimental data showing a “switch-like” feature of responses of a certain populations of neurons in the optic tectum and superior colliculus (Mysore et al., 2011; Jagadisan and Gandhi, 2014). The other critical simplification in our model is in regards to the assumption of shape circularity, and the coincidence of dimensions of Gaussian profiles of attentional windows and relevant neural excitation. In addition, the model does not take into account the potential skewness of the profiles, along the radial direction in the visual field (Ottes et al., 1986). Concerns regarding the shape of the profile do not appear to be crucial in the case of the most elementary one-dimensional stimuli. However, the shape of the profile can significantly impact the results of calculations for more sophisticated filling of two-dimensional illusory figures.

In addition to the simplifications mentioned above, our model did not consider a variety of concomitant neural processes that may influence the assessment of the parameters of the filled-space illusion. For example, the model practically was not concerned with issues related to spatial-frequency filtering, that begins at the lowest anatomical levels of the visual system. Similarly, the role of top-down control from higher-order brain regions is beyond of the scope of the present modeling. In addition, it is important to note that we attempted to implement centroid biases in our calculations, to account for putative manifestation of the modified Müller-Lyer illusion (Bulatov et al., 2009; Bulatov et al., 2010). A direct algebraic summation of the effects presumably caused by stimulus contextual filling and the effects caused by processes of automatic centroid extraction yielded significantly exaggerated values compared to the illusion magnitudes obtained from experiments. Nevertheless, after some examination of computational procedures, we have found that the Muller-Lyer effects can be accounted for via additional modifications of input parameters to the proposed model of the filled-space illusion. However, unfortunately, these modifications substantially complicate the existing equations. Accordingly, one can assume a certain hierarchy in spatial information processing wherein misjudgments caused by contextual filling can be regarded as systematic measurement errors of a “ruler” that is used to assess the metric properties of excitation profiles already altered by processes of automatic centroid extraction.

Our data collected with different stimuli support the idea that spatial pooling of context-evoked neural excitation is one of the main causes of the filled-space illusion. In particular, for a relatively small number of filling dots (n=1-4) in the Oppel-Kundt stimulus, it can be supposed that the profiles of neural excitation caused separately by each filler do not likely show significant overlap. Therefore, according to formula 2, the resulting illusion may be considered simply to be the sum of approximately independent contributions from each distracting dot. Thus, the strength of the Oppel-Kundt illusion (i.e., the fourth set of experiments) with low-density filling should not differ significantly from the sum of the magnitudes of the illusion evoked by a single distractor presented at corresponding positions within the reference interval (i.e., the second set of experiments). It is noteworthy that implementation of the suggestion yields quite comparable values for the grand mean data from the fourth (3.99±0.63, 7.81±0.58, 10.3±0.88, 10.88±0.86 arcmin for the number of fillers equal to one, two, three, and four, respectively) and second set of experiments (3.1±0.31, 7.07±0.47, 9.64±0.58, 12.8±0.61 arcmin for relevant sum of the magnitudes), evidenced by a Wilcoxon signed rank test (Z=0.365, P=0.875).

A number of experimental studies of visual crowding in humans indicate that a limited resolution of spatial attention largely underlies the phenomenon wherein subjects are unable to identify features of objects in visual clutter (Cavanagh and Holcombe, 2007; Fang and He, 2008; Strasburger et al., 2011). Several authors have stressed that one of the key properties of crowding is associated with uncertainty in spatial localization of objects that are closer to each other than the critical spacing, which, in turn, is proportional to retinal eccentricity (Pelli et al., 2004, Strasburger, 2005). Since our model of the filled-space illusion is based on the idea of objects interacting within the limits of some attentional windows that increase in size with eccentricity, we assert that it is reasonable to compare the parameters related to the limited resolution of spatial attention from the present study with the relevant data on crowding reported in the literature. It should be pointed out that this comparison is extremely formal, and concerns only the issue for spatial scaling across eccentricity without any assertions regarding the common ground for neural mechanisms underlying the illusion and crowding. In their experimental study of crowding, Strasburger and Malania (2013) identified a particular target-flanker distance wherein the number of crowding-related spatial localization errors is maximum. Interestingly, this distance scales with eccentricity in a linear manner with the values of slope and intercept equal to 0.188 and 4.2 arcmin, respectively. Remarkably, these data are in good agreement with the slope (k=0.19±0.01) and intercept (s=5.96±1.08 arcmin), which specify a linear dependence on eccentricity for the standard deviation of the Gaussian profile of the attentional window obtained from fitting the model to the grand mean data from the third set of experiments (Table I).

The interpretation of the effects of the Oppel-Kundt illusion proposed by Ganz (1966) can be considered as a possible alternative explanation of our results. The computational procedures of the Ganz model include some calculations of convolution and spatial integration. Therefore, this model is one of a group of theoretical approaches that emphasize the role of neural spatial-frequency filtering in various geometrical illusions (Bulatov et al., 1997; Morgan, 1999; Surkys et al., 2006; Sierra-Vázquez and Serrano-Pedraza, 2007). According to the Ganz model, illusory effects appear due to localization errors that result from lateral inhibition, which specifically modify the profile of neural excitation. Neural excitation changes may thus, in turn, result in a perceptual repulsion of stimulus elements. However, recent experimental data demonstrate that the effects of repulsion can account for only about one-tenth of an actual strength of the Oppel-Kundt illusion (Mikellidou and Thompson, 2014). Nevertheless, as noted by the authors (Mikellidou and Thompson, 2014), there is a still the theoretical possibility of a more substantial contribution from lateral inhibition to the total illusion magnitude. This calls for a more careful accounting of gaze fixation parameters of the subject.

Due to the properties of the calculation procedures used, our model of the filled-space illusion can also be formally considered as representing to some degree the spatial-frequency filtering hypothesis. This hypothesis suggests that misperceptions of stimulus extent are caused by positional biases of specific loci in the profile of neural excitation. Our model, in contrast, interprets the effects of the illusion in terms of context-modified activity of some hypothetical visual subsystem of encoding of retinotopic coordinates, caused by the magnitude of neural response. An adequate correspondence between experimental results and the predictions of our model led us to conclude that visual information processing in superficial layers of the superior colliculus can, to a large extent, be responsible for the effects of the filled-space illusion. Indeed, there is wide consensus in the literature that these layers of the superior colliculus play a key role in gaze control, and that elevated activity of neuronal population in their maps encode the retinotopic distance to a visual target (Klier et al., 2001; Bergeron et al., 2003; Nakahara et al., 2006; Krauzlis et al., 2013; Vokoun et al., 2014; Taouali et al., 2015).

The present study used elementary stimuli that consisted of single-dot distractors distributed along a single stimulus axis. Similarly, we considered only the simplest one-dimensional features of the filled-space illusion. Therefore, further development of the model is needed to account for data collected from experiments with more sophisticated two-dimensional stimuli, which comprise the filling of different shape or luminance contrast.

CONCLUSIONS

The aim of the present study was to further develop our computational model of the filled-space illusion and examine whether the model equations are applicable for fitting experimental data collected for stimuli comprising single-dot distractors. In three sets of experiments, we investigated the illusory effect as a function of distance between the distractor and lateral terminator of the reference spatial interval of the horizontal three-dot stimulus. We found that our model predictions adequately fit all variations of the illusion magnitude for distracting dots placed both outside and inside the interval, as well as, for two distractors arranged symmetrically relative to the terminator. The applicability of our model was additionally confirmed by successful fitting to data collected in experiments using the conventional Oppel-Kundt figures. Adequate correspondence between the experimental and theoretical results supports the idea that the filled-space illusion can be caused, in part, by perceptual positional biases induced by the context-evoked increase in neural excitation.

REFERENCES

Bailes SM (1995) Effects of processing time and stimulus density on apparent width of the Oppel-Kundt illusion [PhD Thesis]. Concordia University, Montréal, QC, CA.

Beck J, Rosenfeld A, Ivry R (1989) Line segregation. Spat Vis 4: 75–101.

Bergeron A, Matsuo S, Guitton D (2003) Superior colliculus encodes distance to target, not saccade amplitude, in multi-step gaze shifts. Nature Neurosci 6: 404−413.

Bertulis A, Bulatov A (2001) Distortions of length perception in human vision. Biomedicine 1: 3–23.

Bertulis A, Surkys T, Bulatov A, Bielevičius A (2014) Temporal dynamics of the Oppel-Kundt Illusion compared to the Müller-Lyer illusion. Acta Neurobiol Exp 74: 443–455.

Bulatov A, Bertulis A (1999) Distortions of length perception. Biol Cybern 90: 185–193.

Bulatov A, Bertulis A (2005) Superimposition of illusory patterns with contrast variations. Acta Neurobiol Exp 65: 51–60.

Bulatov A, Bertulis A, Bulatova N (2005) Discrimination of a right angle with monocular and cyclopic perception. Human Physiology 31: 381–391.

Bulatov A, Bertulis A, Bulatova N, Loginovich Y (2009) Centroid extraction and illusions of extent with different contextual flanks. Acta Neurobiol Exp 69: 504−525.

Bulatov A, Bertulis A, Gutauskas A, Mickiene L, Kadziene G (2010) Center-of-mass alterations and visual illusions of extent. Biol Cybern 102: 475−487.

Bulatov A, Bertulis A, Mickienė L (1997) Geometrical illusions: study and modelling. Biol Cybern 77: 395–406.

Bulatov A, Bulatova N, Surkys T, Mickienė L (2017) An effect of continuous contextual filling in the filled-space illusion. Acta Neurobiol Exp 77: 157−167.

Carandini M, Heeger DJ (2012) Normalization as a canonical neural computation. Nat Rev Neurosci 13: 51−62.

Cavanagh P, Holcombe AO (2007) Non-retinotopic crowding. J Vis 7: 338.

Coren S, Girgus JS, Ehrlichman H, Hakistan AR (1976) An empirical taxonomy of visual illusions. Percep Psychophys 20: 129−147.

Coren S, Hoenig P (1972) Eye movements and decrement in the Oppel-Kundt illusion. Percep Psychophys 12 : 224−225.

Craven BJ, Watt RJ (1989) The use of fractal image statistics in the estimation of lateral spatial extent. Spat Vis 4: 223−239.

Deregowski JB, McGeorge P (2006) Oppel-Kundt illusion in three-dimensional space. Perception 35: 1307−1314.

Dworkin L, Bross M (1998) Brightness contrast and exposure time effects on the Oppel-Kundt illusion. Percept Suppl 27: 87.

Erdfelder E, Faul F (1994) A class of information integration models for the Oppel-Kundt illusion (in German). Z Psychol Z Angew Psychol 202: 133–160.

Eriksson ES (1970) A field theory of visual illusions. Br J Psychol 61: 451−466.

Fang F, He S (2008) Crowding alters the spatial distribution of attention modulation in human primary visual cortex. J Vis 8: 1–9.

Field DJ, Hayes A, Hess RF (1993) Contour integration by the human visual system: Evidence for a local "association field". Vision Res 33: 173–193.

Ganz L (1966) Mechanism of the figural aftereffects. Psychol Review 73: 128–150.

Giora E, Gori S (2010) The perceptual expansion of a filled area depends on textural characteristics. Vision Res 50: 2466–2475.

Hirsch J, DeLaPaz RL, Relkin NR, Victor J, Kim K, Li T, Borden P, Rubin N, Shapley R (1995) Illusory contours activate specific regions in human visual cortex: evidence from functional magnetic resonance imaging. Proc Natl Acad Sci USA 92: 6469–6473.

Jagadisan UK, Gandhi NJ (2014) Neural mechanisms of target selection in the superior colliculus. In: The new visual neurosciences (Chalupa LM, Werner JS, Eds). MIT Press, Cambridge, USA, p. 921–934.

Klier EM, Wang H, Crawford JD (2001) The superior colliculus encodes gaze commands in retinal coordinates. Nat Neurosci 4: 627–632.

Kojo I, Liinasuo M, Rovamo J (1993) Spatial and temporal properties of illusory figures. Vision Res 33: 897–901.

Krauzlis RJ, Lovejoy LP, Zènon A (2013) Superior colliculus and visual spatial attention. Annu Rev Neurosci 36: 165–82.

Krauzlis RJ, Goffart L, Hafed ZM (2017) Neuronal control of fixation and fixational eye movements. Phil Trans R Soc B 372: 20160205.

Lewis EO (1912) The illusion of filled space. Brit J Psychol 5: 36–50.

Long GM, Murtagh MP (1984) Task and size effects in the Oppel–Kundt and irradiation illusions. J Gen Psychol 111: 229–240.

Mikellidou K, Thompson P (2014) Crossing the line: estimations of line length in the Oppel-Kundt illusion. J Vis 14: 20.

Morgan MJ (1999) The Poggendorff illusion: a bias in the estimation of the orientation of virtual lines by second-stage filters. Vis Res 39: 2361−2380.

Mysore SP, Asadollahi A, Knudsen EI (2011) Signaling of the strongest stimulus in the owl optic tectum. J Neurosci 31: 5186−5196.

Nakahara H, Morita K, Wurtz RH, Optican LM (2006) Saccade-related spread of activity across superior colliculus may arise from asymmetry of internal connections. J Neurophysiol 96: 765–774.

Noguchi K (2003) The relationship between visual illusion and aesthetic preference-an attempt to unify experimental phenomenology and empirical aesthetics. Axiomathes 13: 261–281.

Noguchi K, Hilz R, Rentschler I (1990) The effect of grouping of adjacent contours on the Oppel-Kundt illusion (in Japanese). Jpn J Psychon Sc 8: 57–60.

Obonai T (1933) Contributions to the study of psychophysical induction: III. Experiments on the illusions of filled space. Jpn J Psychol 8: 699–720.

Obonai T (1954) Induction effects in estimates of extent. J Exp Psychol 47: 57–60.

Olsen SR, Bhandawat V, Wilson RI (2010) Divisive normalization in olfactory population codes. Neuron 66: 287–299.

Ottes FP, Gisbergen JAM, Eggermont JJ (1986) Visuomotor fields of the superior colliculus: a quantitative model. Vision Res 26: 857–873.

Oyama T (1960) Japanese studies on the so-called geometrical-optical illusions. Psychologia 3: 7–20.

Pelli DG, Palomares M, Majaj NJ (2004) Crowding is unlike ordinary masking: Distinguishing feature integration from detection. J Vis 4: 1136–1169.

Piaget J, Bang V (1961) The evolution of the illusion of divided extent (Oppel-Kundt) in the tachistoscopic presentation (in French). Arch Psychol 38: 1–21.

Piaget J, Osterrieth PA (1953) Research on the development of perceptions: XVII. The evolution of the Oppel-Kundt illusion as a function of age (in French). Arch Psychol 34: 1–38.

Reynolds JH, Heeger DJ (2009) The normalization model of attention. Neuron 61: 168–185.

Robinson JO (1998) The psychology of visual illusion. Dover Publications, New York, USA.

Sierra-Vázquez V, Serrano-Pedraza I (2007) Single-band amplitude demodulation of Müller-Lyer illusion images. Spanish J Psychol 10: 3−19.

Smits JT, Vos PG, Oeffelen MP van (1985) The perception of a dotted line in noise: a model of good continuation and some experimental results. Spat Vis 1: 163–177.

Spiegel HG (1937) On the influence of the intermediate field on visually assessed distances (in German). Psychol Forsch 21: 327–383.

Strasburger H (2005) Unfocussed spatial attention underlies the crowding effect in indirect form vision. J Vis 5: 1024–1037.

Strasburger H, Rentschler I, Jüttner M (2011) Peripheral vision and pattern recognition: A review. J Vis 11: 13.

Strasburger H, Malania M (2013) Source confusion is a major cause of crowding. J Vis 13: 24.

Surkys T, Bertulis A, Bulatov A (2006) Delboeuf illusion study. Medicina (Kaunas) 42: 673–681.

Surkys T (2007) Influence of colour and luminance contrast on perceptual distortions of stimulus geometry [PhD Thesis]. Kaunas University of Medicine, Kaunas, LT.

Taouali W, Goffart L, Alexandre F, Rougier NP (2015) A parsimonious computational model of visual target position encoding in the superior colliculus. Biol Cybern 109: 549–559.

Taylor MM (1962) Geometry of a visual illusion. J Opt Soc Am 52: 565–569.

Vokoun CR, Huang X, Jackson MB, Basso MA (2014) Response normalization in the superficial layers of the superior colliculus as a possible mechanism for saccadic averaging. J Neurosci 34: 7976–7987.

Wackermann J (2012a) Determinants of filled/empty optical illusion: Differential effects of patterning. Acta Neurobiol Exp 72: 89–94.

Wackermann J (2012b) Determinants of filled/empty optical illusion: Influence of luminance contrast and polarity. Acta Neurobiol Exp 72: 412–420.

Wackermann J, Kastner K (2009) Paradoxical form of filled/empty optical illusion. Acta Neurobiol Exp 69: 560–563.

Wackermann J, Kastner K (2010) Determinants of filled/empty optical illusion: search for the locus of maximal effect. Acta Neurobiol Exp 70: 423–434.

Watt RJ (1990) The primal sketch in human vision. In: AI and the Eye (Blake A, Troscianko T, Eds.). J Wiley and Sons, New York, p. 147–180.